Planetary and Space Science 59 (2011) 292–298

Contents lists available at ScienceDirect

Planetary and Space Science

journal homepage: www.elsevier.com/locate/pss

Studying methane and other trace species in the Mars atmosphere using a SOIR instrument

R. Drummond *, A.-C. Vandaele, F. Daerden, D. Fussen, A. Mahieux, L. Neary, E. Neefs, S. Robert, Y. Willame, V. Wilquet

BIRA-IASB, Ringlaan 3, 1180 Ukkel, Belgium

ARTICLE INFO

Article history:
Received 2 March 2010
Received in revised form
30 April 2010
Accepted 14 May 2010
Available online 24 May 2010

Keywords:
Planetary atmospheres
IR spectroscopy
AOTF
Mars

ABSTRACT

Solar Occultation in the InfraRed (SOIR) is one of three spectrometers of the SPICAV/SOIR instrument suite (Bertaux et al., 2007b) on board the Venus Express orbiter (VEX). VEX has been in orbit around Venus since April 2006 and to date SOIR has carried out over 674 measurements. Pre-launch and in-orbit performance analyses allow us to predict what SOIR would be capable of at Mars. SOIR spectra through the Martian atmosphere have been simulated with ASIMUT, a line-by-line (LBL) radiative transfer code also used for the retrieval of vertical profiles of atmospheric constituents of Venus (Vandaele et al., 2008; Bertaux et al., 2007a). The code takes into account the temperature and pressure vertical profiles as well as those of the atmospheric species, but also the instrument function and the overlapping of the diffraction orders of the echelle grating. We will show these spectra and the detection limits of species that could be studied using a SOIR spectrometer making solar occultation or nadir measurements in Mars orbit.

1. Introduction

The recent reports of methane detection on Mars (Formisano et al., 2004; Krasnopolsky et al., 2004; Mumma et al., 2004) may prove, if confirmed, that Mars is a much more active planet than previously assumed. The reported spatio-temporal variability (Mumma et al., 2009) hints at recent and localized production, e.g. by outgassing, while the destruction of methane seems incompatible with classic photochemical processes (Lefevre and Forget, 2009). Only additional high-quality observations, preferentially from Mars orbit, will allow us to eventually solve the enigma. The SOIR spectrometer offers a high spectral resolution at moderate mass, proven heritage on a planetary mission, and flexibility in operation modes. Besides the original solar occultation mode, the compactness of the instrument allows for a nadir viewing mode which would enable a detailed and simultaneous characterisation of the spatio-temporal distribution of methane and other species. We examine in this paper the potential capability of a SOIR instrument at Mars, as well as a modified version for nadir observations. Future missions to Mars could fly two SOIR channels, or use the more sensitive SOIR to cover both options.

SOIR, an Echelle infrared spectrometer using an acousto-optic tunable filter (AOTF) for the order selection, has been in orbit around Venus on ESA's Venus Express mission since April 2006 and to date SOIR has carried out over 674 measurements (271 occultations and 403 calibration measurements) (Mahieux et al., 2008; Wilquet et al., 2009). SOIR probes the atmosphere of Venus by solar occultation, operating between 2.2 and 4.3 μm, with a resolution of 0.1–0.2 cm^{-1}. This spectral range is suitable for the detection of several key components of planetary atmospheres in general, including CO_2 and its isotopologues (Vandaele et al., 2007; Bertaux et al., 2008; Wilquet et al., 2008), H_2O and its isotopologue HDO (Fedorova et al., 2008), CH_4, CH_2O, SO_2 (Belyaev et al., 2008), HCl, and other trace species. SOIR hence offers a unique potential to follow-up on the issue of Martian methane, not only by the direct detection of CH_4 down to sub parts per billion level (see Section 4), but also by the quasi-simultaneous detection of chemical and physical components which may be closely related to its origin and destruction such as H_2O, SO_2, H_2CO, dust and ice clouds.

The SOIR instrument was designed to have a minimum of moving parts (Nevejans et al., 2006); and to be light and compact. The AOTF allows a narrow range of wavelengths to pass, according to the radio frequency of the acoustic wave applied to the TeO_2 crystal; this selects the order. The advantage of the AOTF is that different orders can be observed quickly and easily during one occultation. To obtain a compact optical scheme, a Littrow configuration was implemented in which the usual collimating

* Corresponding author. Tel.: +32 2 3730475; fax: +32 2 3738423.
E-mail address: rachel.drummond@aeronomie.be (R. Drummond).

0032-0633/$ - see front matter © 2010 Elsevier Ltd. All rights reserved.
doi:10.1016/j.pss.2010.05.009

and imaging lenses are merged into a single off-axis parabolic mirror. The light is diffracted on the echelle grating, where orders overlap and addition occurs, and finally is recorded by the detector. The detector is 320×256 pixels and is cooled to 88 K to maximise the signal to noise ratio.

2. Orbital coverage and resolution

2.1. Coverage

The ExoMars Trace Gas Mapper mission announced for 2016 will be placed in a 400 km altitude circular orbit at $74\pm10^{\circ}$ inclination (NASA and ESA, 2010). We looked at the solar occultation coverage for 74°, as well as 84° and 64°. These alter the number of solar occultations within a Martian year as well as the range of latitudes scanned as seen in Fig. 1. From a 74° inclined orbit, the latitudes covered range from −87 to +88 with good revisit time at various solar longitudes. This would allow SOIR to obtain vertical profiles of major and minor constituents for northern and southern hemispheres during each Martian season. A higher inclination orbit gives us access to occultations at higher latitudes but less frequent occultations, whereas the lower inclination increases the number of occultations but decreases the latitude coverage range.

The nadir coverage depends on inclination also, since we cannot observe beyond $\pm i$ degrees, where i is the inclination. The coverage varies throughout the year, as can be seen in Fig. 2. We show the nadir coverage for two different days from the 74°, 400 km orbit. The rotation of Mars and the precession of the orbit displaces the ground track a little each orbit. This would allow SOIR to pinpoint local sources of methane and to constrain the displacement and possible destruction of any methane plumes.

2.2. Spatial resolution

For SOIR/VEX we routinely achieve a spatial resolution of less than 500 m, meaning a layer of 500 m of the atmosphere is scanned during one recording. This depends primarily on the vertical speed of the satellite with respect to the line of sight to the Sun and the atmospheric layer being sounded. At 400 km the orbital velocity of a satellite is $\sqrt{GM/a}\approx3.4\,\mathrm{km\,s^{-1}}$. The worst vertical resolution at the limb occurs towards the end of occultations in the orbital plane when the apparent speed of the tangent height is about 1.5 km/s, or 375 m for a nominal integration time of 250 ms. This integration time should remain the same since the radiance we receive at Mars is the same as the radiance at Venus. At Mars the Sun subtends 21′, a value smaller than the angular field of the current SOIR slit ($30'\times2'$). This means that fewer pixel rows can be summed to give us a

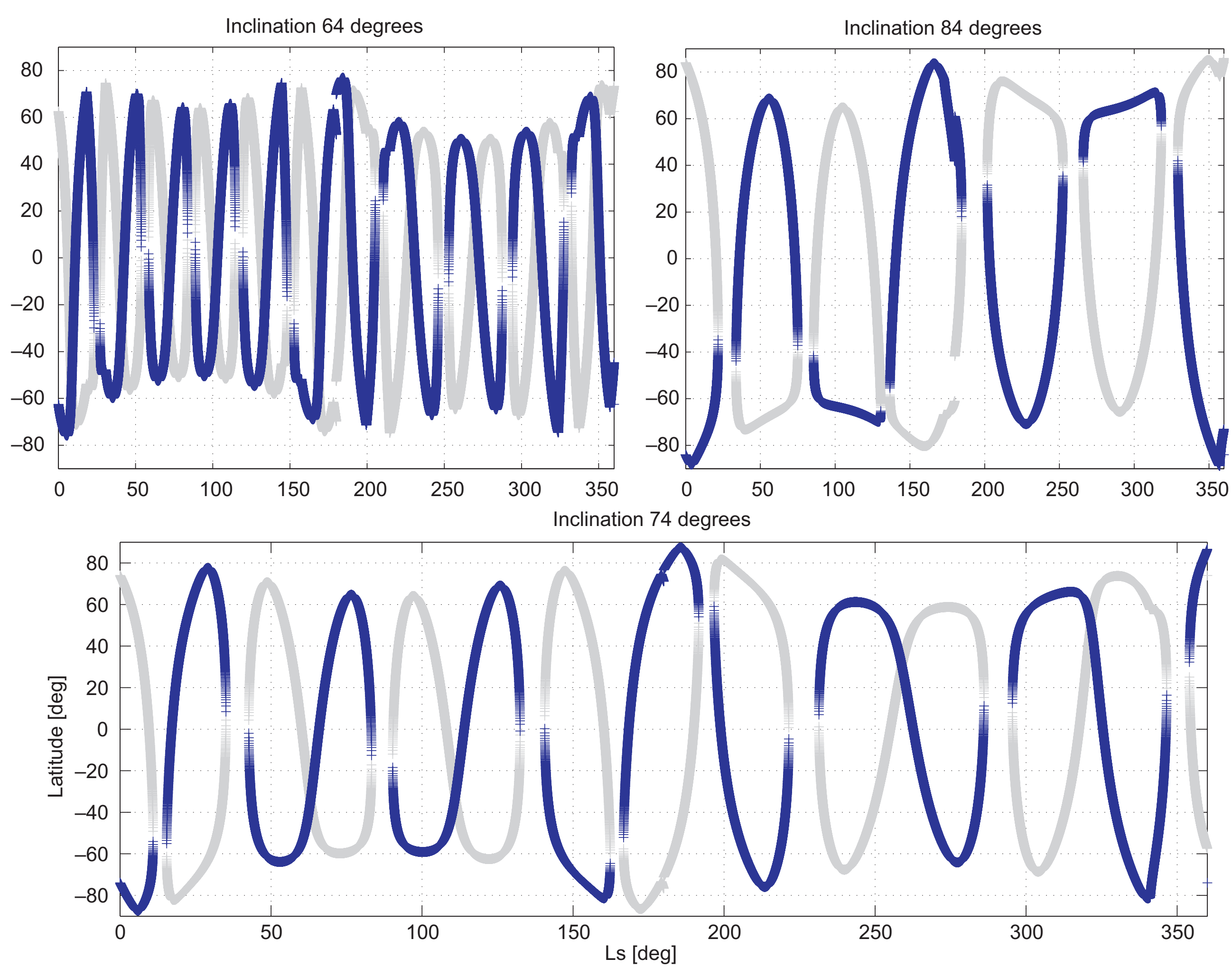

Fig. 1. Latitudes of tangent points in solar occultation versus the solar longitude Ls (360° = 1 Martian year). These were simulated for the ascending node starting at the vernal point.

spectrum, reducing slightly our signal to noise ratio. This can be compensated for by the various instrumental improvements discussed in Section 3.

Nadir observations will receive less total light, specifically a factor of $(r_{Sun}/r_{Mars})^2$*.Albedo* where r_{Sun} is the radius of the Sun and r_{Mars} is the distance from the planet to the Sun. The albedo is the reflectance of the surface of Mars, which depends on the area of Mars as well as the season and the wavelength. An average value of 0.15 was used here. This gives a reduction in light of $(6.96\times10^5/2.28\times10^8)^2\times0.15=1.4\times10^{-6}$ (for SZA=0°). This reduction in signal can be compensated for by a larger slit and various other techniques, discussed in Section 3. We can increase the slit long edge from 30′ to 100′ (3 times more signal) and still use the same optics. We can also increase the slit in the spectral direction, from 2′ to 8′. This would decrease our spectral resolution slightly (0.4–0.8 cm^{-1}), but would allow 4 times more light in. For nadir observations our spatial resolution is given by $Altitude\times2\times tan(FOV/2)$. So with the current slit size, in a 400 km orbit we have an instantaneous resolution of 3.5 km by 0.23 km. At 3.4 km s^{-1} we can therefore accumulate (co-add) for 174 s before reaching a 10° latitudinal bin.

3. Instrumental improvements

One of the principal advantages in having a version of SOIR already in space is that we can learn from the observations already ongoing. The results from SOIR/VEX are excellent, but improvements are still possible, especially to deal with new challenges posed by a Mars mission and the nadir development. One such improvement would be the use of an AOTF with side-lobe suppression. On SOIR/VEX the AOTF transfer function has irregular side lobes that cause order pollution by folding in absorption lines in neighbouring orders. The issue of side lobes, how we measure and correct for the effect is discussed at length in Mahieux et al. (2009). Having new AOTFs with side-lobe suppression would facilitate the retrieval for both the solar occultation and nadir channels. A new AOTF with a wider étendue would also allow more light into the optics and increase our SNR; matching the *f* number of the optics would also increase throughput. However the major change would consist in minimising the thermal background seen by a nadir version of the instrument. This can be done by cooling the optics after the slit and by restricting the spectral range of the detector by inserting a cold filter in front of the focal plane array. This would significantly

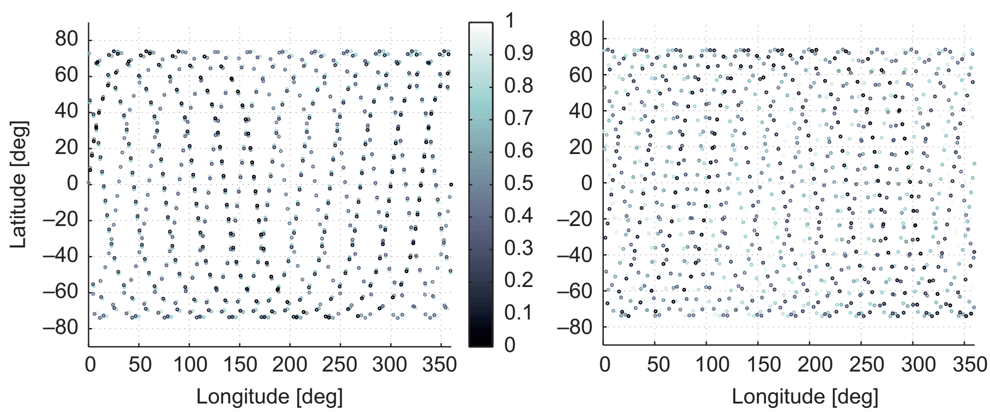

Fig. 2. This shows the nadir coverage for days 1 (left) and 10 (right) from the orbit at 74° inclination and 400 km. The ascending node starts at the vernal equinox for this simulation and processes eastward. The colour scale shows how the ground track evolves within the day.

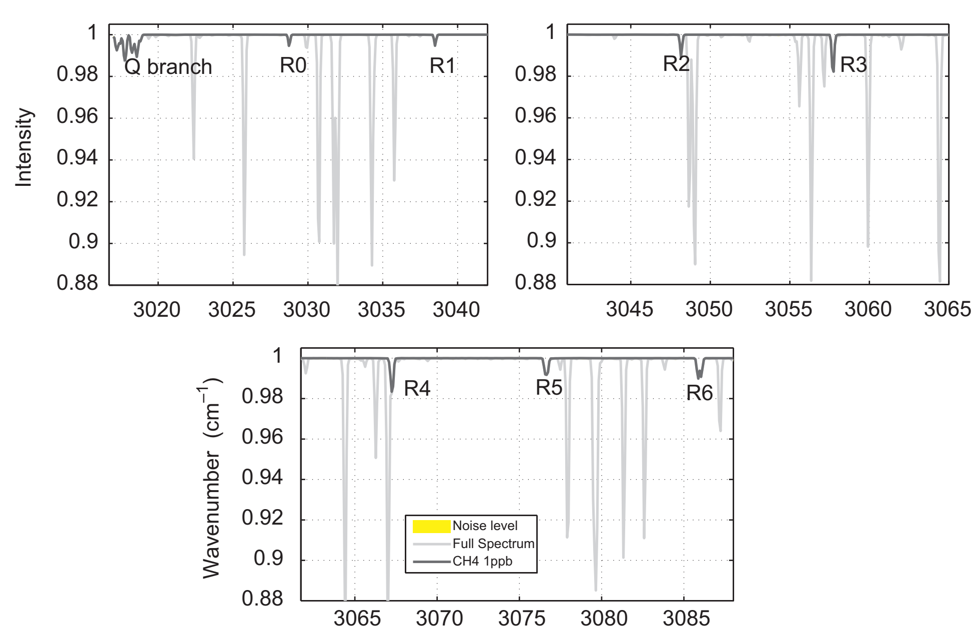

Fig. 3. Simulated solar occultation spectra for three orders where methane absorbs. The other lines come mainly from H_2O but also from CO_2.

increase the signal to noise ratio on the nadir channel, since at 273 K the thermal background across the entire SOIR spectral range amounts to $9.4\times10^{7}\,e^{-}\,s^{-1}\,pixel^{-1}$. This can be reduced by a factor 10 by cooling to 233 K and to $3.7\times10^{5}\,e^{-}\,s^{-1}\,pixel^{-1}$ at 193 K. If we can cool as far as 173 K then we have a factor of 2180 less thermal background. If we also cut-off the range of sensitivity of the detector at 3.8 μm, the thermal background at 173 K is reduced to less than $1\times10^{4}\,e^{-}\,s^{-1}\,pixel^{-1}$. These improvements give the nadir instrument a signal to noise ratio of 68 at 3.0 μm with a narrow slit (high resolution). If we bin together 100 pixels in the spatial direction (our longer slit size), we have an SNR of 682.

4. Simulations

We have simulated measurements using a model atmosphere from the Mars Global Circulation Model GM3 or GEM-Mars (Moudden and McConnell, 2005) which was run for two consecutive Martian years. It starts from uniform initial conditions with the chemistry scheme of Garcia Munoz et al. (2005), implemented online and with smoothed averaged TES dust load conditions (Smith, 2004). We used averaged temperature, pressure and water vapour profiles for Ls = 180° at northern mid latitudes. We use ASIMUT, a line-by-line radiative code, configured for the viewing geometry of

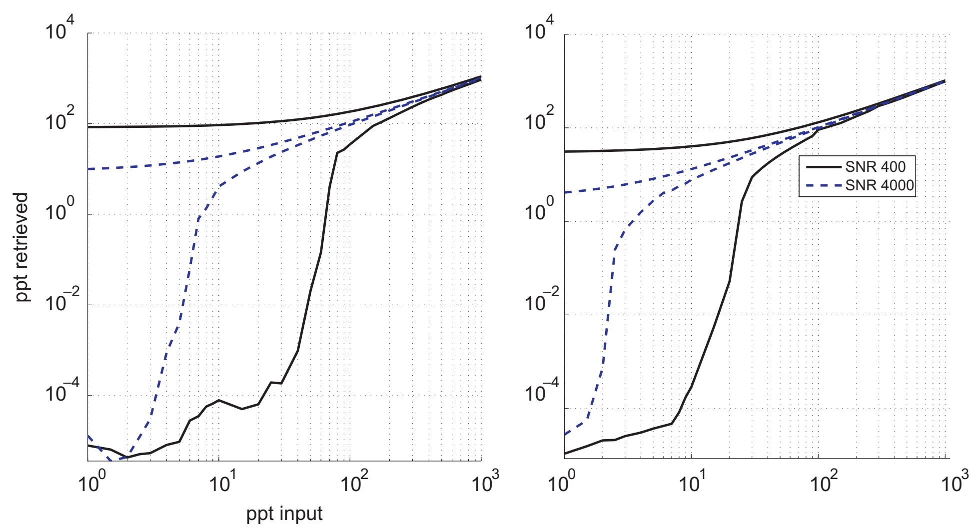

Fig. 4. The 3-sigma confidence limits on the retrieval of a given CH_4 concentration from a solar occultation spectrum for SNRs of 400 and 4000. Left: Fit of only the methane Q-branch. Right: Fit over a larger spectral window.

Table 1
Detection limits for SOIR in solar occultation mode for an SNR of 4000 and in nadir mode for an SNR of 700.

Species	Scientific objective	Current knowledge	Detection limit	
			SO	Nadir
CH_4	Identify sources	0–60 ppb[a]	10 ppt	0.1–1 ppb
H_2O	Profile abundance	< 300 ppm (variable with season)[c,d,e]	2 ppb	8 ppb
CO	Profile concentration	700–800 ppm[f]	15 ppb	0.1–1 ppm
HDO	Profiling isotopic ratios	0.85 ppm[g]	30 ppb	5 ppb
$^{13}CO_2$		ratios wrt Earth[d,h]		
^{17}OCO		$^{13}C/^{12}C = 0.94$		
^{18}OCO		$^{17}O/^{16}O = 0.95$		
$C^{18}O_2$		$^{18}O/^{16}O = 0.90$		
Aerosol	Properties, extinction profiles	MGS TES opacities, integrated and limb profiles ($\Delta z \sim 5$ km)[b]		
H_2CO	Search for unidentified species	< 3 ppb[i]	0.2 ppb	0.1–1 ppb
C_2H_6		< 400 ppb[j]	0.05 ppb	0.1–1 ppb
HCl		< 2 ppb[i]	0.05 ppb	2 ppb
HCN			0.1 ppb	5 ppb
H_2S		< 100 ppb[i]	6 ppb	0.1 ppm
HO_2			10 ppb	50 ppb
OCS		10 ppb[j]	0.8 ppb	20 ppb
SO_2		1 ppb[i]	50 ppb	0.1 ppm

The nadir calculation assumes a constant vmr. References for current knowledge.

[a] Mumma et al. (2007).
[b] Smith (2004).
[c] Lissauer and DePater (2001).
[d] Encrenaz et al. (2005).
[e] Encrenaz et al. (2006).
[f] Chamberlain and Hunten (1987).
[g] Lodders and Fegley (1997).
[h] Krasnopolsky (1996).
[i] Krasnopolsky (2010).
[j] MSO Science Objectives Report.

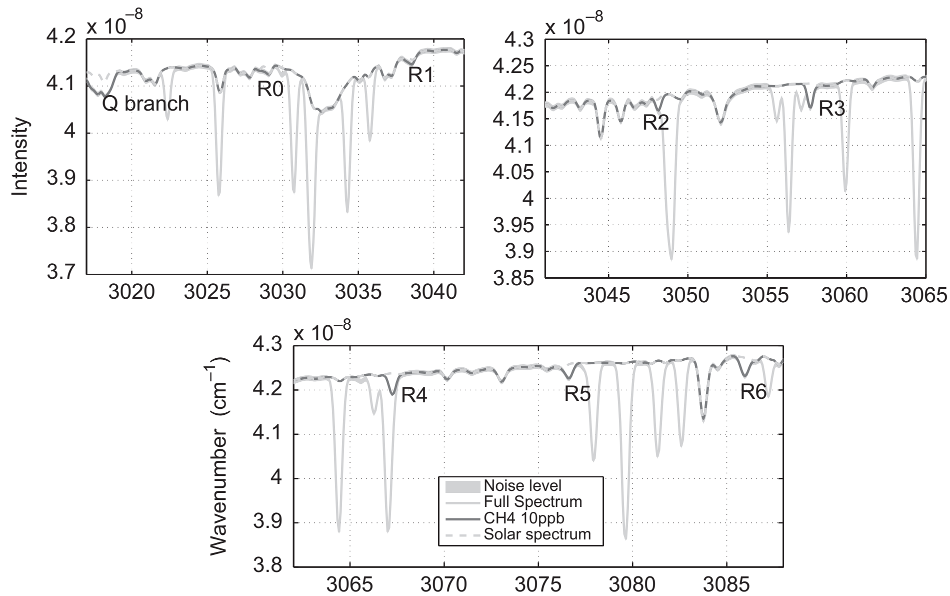

Fig. 5. Simulated nadir spectra for three orders where methane absorbs. Here the contribution from the solar spectrum is also highlighted.

the proposed ExoMars 2016 Orbiter. We took standard values of the carbon dioxide concentrations and then added methane at various concentrations to assess the SOIR instrument sensitivity. Tests were also run with ozone, since it absorbs at similar wavenumbers, but this did not disrupt the detection of methane until the input volume mixing ratio reached unrealistic levels.

4.1. Solar occultation

Solar occultation measurements are shown in Fig. 3, computed as the ratio of the measured spectrum and the exo-atmosphere solar spectrum (transmittance). This removes the problem of solar absorption lines and instrument sensitivity calibration. The signal to noise ratio used for this plot is 2000, a value we routinely achieve with SOIR on VEX. A 1 ppb level of CH_4 was chosen to make it clear on the plot. These simulated spectra were used in a further study of detectability. Representative noise levels were added to the spectra and a retrieval performed assuming no prior knowledge of the concentration. Fig. 4 shows the confidence limits on retrieving various input concentrations with signal to noise ratios of 400 and 4000 and fits on just the Q-branch or a wider spectral window. This shows that concentrations below 1 ppb can be detected from just one spectrum. Since SOIR can take several spectra per second in occultation, we can increase the detection limit. It would therefore be possible to go below a 10 ppt detection limit with averaging. This is also shown in Table 1, which covers far more than just the methane detectability, since SOIR's spectral range allows it to tackle much more science. SOIR can obviously improve CH_4 concentration measurements and maps, but can also provide data for photo-chemical loss investigations (water isotopologues). CO and aerosol profiles would provide sampling for GCM model constraints; profiles of isotopic ratios of various molecules would greatly enhance the knowledge base compared to Earth's ratios and detection; confirmation and mapping of species as yet unidentified in the Martian atmosphere are also important.

4.2. Nadir

Fig. 5 shows a simulated nadir observation of methane. An input solar spectrum was taken (Hase et al., 2009) for the

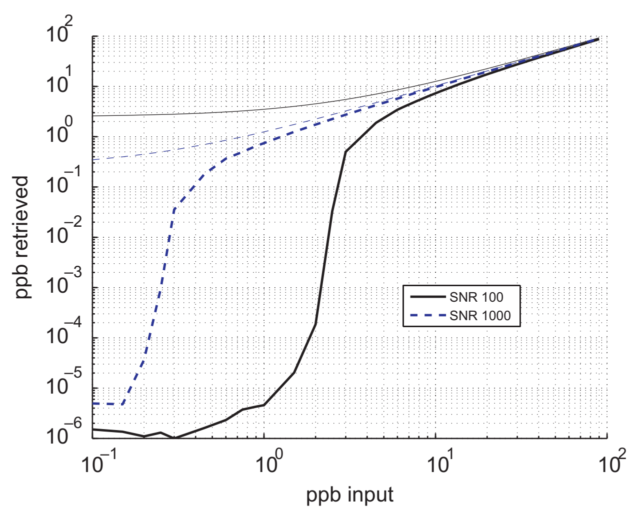

Fig. 6. The 3-sigma confidence intervals on the retrieved methane concentration for the Q-branch in nadir spectra (assuming no prior knowledge) for SNRs of 100 and 1000.

wavelength range covered by SOIR. The black body emission of the surface of Mars at representative temperatures was included, as well as emission from atmospheric layers. The resolution was lowered to an indicative value of 0.4 cm^{-1} to demonstrate that we can still detect methane at this resolution. The detection limit was studied further in a similar way to the solar occultation study, by simulating spectra for several atmospheric altitudes, but without aerosols. Representative noise sources were then added, to simulate various signal to noise ratios. The spectra obtained were inverted to retrieve CH_4 profiles which are compared to the input profile. Results for signal to noise levels of 100 and 1000 are shown in Fig. 6. This shows that for an atmospheric concentration of 1 ppb, at SNR 100 we could retrieve anywhere between 0.01 ppt and 3 ppb, whereas an SNR of 1000 constrains the retrieval to between 0.7 and 1.3 ppb. The confidence interval on an input concentration of 10 ppb is better, of course. As described in Section 3, the improved, cooled design provides an SNR of almost 700 at high resolution, increasing to 4600 at lowered resolution. The nadir detection limits shown in Table 1 are for an SNR of 700

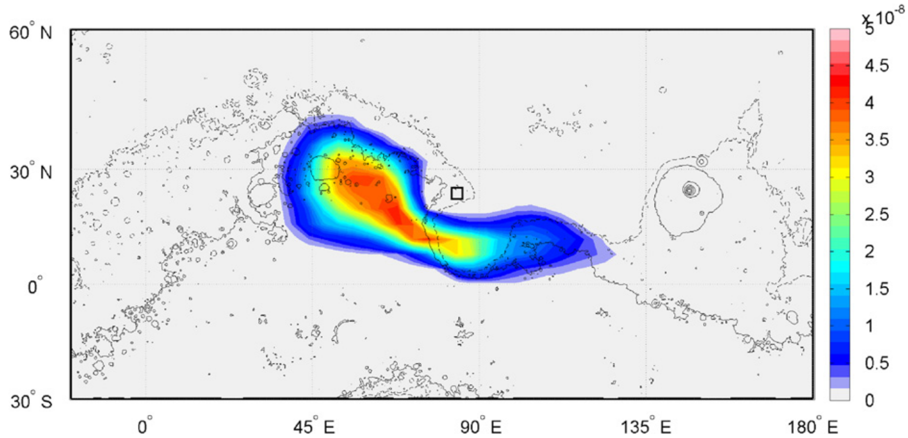

Fig. 7. CH_4 column fraction 5 sols after an impulsive release at Nili Fossae (source location indicated by the square) as calculated by GEM-Mars.

and a resolution of $0.15\,cm^{-1}$. The trade-off between resolution and SNR is a complicated issue, since higher SNR would be better if there is very little methane, whereas higher resolution would allow us to separate out isotopologue lines for CH_4 if the abundance is high enough. A compromise could be a lollypop shaped slit, with a high resolution section and a low resolution section. This way SOIR could identify methane at high resolution by using longer integration times to maximise SNR, then map the methane at low resolution, using shorter integration times to increase the spatial sampling.

5. GCM support for interpretation

Mars global circulation models (GCMs) are an interesting tool to test the evolution of emitted tracers throughout the atmosphere, e.g. Lefevre and Forget (2009). Various tracer emission schemes can be set up (impulsive, slow, over small or large areas etc) at rates inspired by the, to this day sparse, observational data (Mumma et al., 2009). In general the vertical mixing of an emitted tracer occurs very rapidly throughout the planetary boundary layer (PBL) on Mars. The PBL height is typically of the order of 5 km and the strong daytime mixing redistributes dust and vapours uniformly throughout the PBL over a few hours (Whiteway et al., 2009; Daerden et al., 2010). Once the tracer reaches the PBL top, global circulation takes over. Both the transport throughout the PBL and the global circulation can be accurately simulated by GCMs e.g. Moudden and McConnell (2005); Neary et al. (2010).

The SOIR instrument in a continuous nadir viewing mode from a low near-circular orbit will be able to line up the spatial patterns in the methane vertical column distribution with high spatio-temporal precision. Comparing GCM simulations of various emission scenarios with the detected methane maps will allow us to address the likelihood of the emission scenarios, to search for the source regions and to derive emission rates. This search will be refined by techniques such as inverse modelling and chemical data assimilation (Errera et al., 2008).

We programmed several methane emission schemes into the GEM-Mars GCM (Moudden and McConnell, 2005). As an example, we present here the result of an impulsive release over Nili Fossae (indicated as a possible source region by Mumma et al. (2009)), in which 6.2×10^6 kg of methane was released from the surface in 30 min during local daytime; this is 1/3 of the total combined amount of methane in the 3 plumes reported by Mumma et al. (2009). Fig. 7 shows the modelled methane plume 5 sols after release. Due to zonal winds and the influence of the topography the plume does not spread out uniformly in all directions; it is even not located over the source anymore. Such calculations may help to find outgassing source regions and understand the trace gas patterns observed by SOIR.

Besides sources, the sinks of trace gases such as methane can be also studied with Mars GCMs. Inspired by terrestrial modelling efforts for ozone destruction (Daerden et al., 2007), one can implement heterogeneous chemistry on dust and/or ice particles (Lefevre et al., 2008) as a possible cause for methane destruction and verify whether this would be consistent with the observational data on lifetime and the measured spatio-temporal patterns. Other options can also be studied by GCMs, e.g. destruction through interaction with the regolith or in electrochemical processes in dust storms (Atreya et al., 2007).

6. Conclusion

SOIR has already proved its capability in solar occultation at Venus. The developments and improvements made to adapt SOIR to nadir viewing are well defined and feasible. The mystery of methane sources and sinks at Mars is ripe for the solving. An instrument capable of retrieving vertical profiles of molecules during occultations and mapping their location and concentration via nadir viewing would greatly improve our knowledge of the atmosphere of Mars. SOIR for Mars is such an instrument. It is a performant solar occultation and nadir instrument with low accommodation demands on a satellite. We believe that a SOIR instrument on a mission to Mars would solve the mystery of Martian methane.

Acknowledgements

The research program was supported by the Belgian Federal Science Policy Office and the European Space Agency (ESA, PRODEX program, contracts C 90268, 90113, and 17645).

References

Atreya, S., Mahaffy, P., Wong, A.-S., 2007. Methane and related trace species on Mars: origin, loss, implications for life, and habitability. Planet. Space Sci. 55, 358–369.

Belyaev, D., Korablev, O., Fedorova, A., Bertaux, J.-L., Vandaele, A.-C., Montmessin, F., Mahieux, A., Wilquet, V., Drummond, R., 2008. First observations of SO_2

above Venus' clouds by means of solar occultation in the infrared. J. Geophys. Res., doi:10.1029/2008JE003143.

Bertaux, J., Nevejans, D., Korablev, O., Villard, E., Quémerais, E., Neefs, E., Montmessin, F., Leblanc, F., Dubois, J., Dimarellis, E., 2007a. SPICAV on Venus Express: three spectrometers to study the global structure and composition of the Venus atmosphere. Planet. Space Sci. 55 (12), 1673–1700.

Bertaux, J.-L., Vandaele, A., Korablev, O., Villard, E., Fedorova, A., Fussen, D., Quémerais, E., Belyaev, D., Mahieux, A., Montmessin, F., Müller, C., Neefs, E., Nevejans, D., Wilquet, V., Dubois, J., Hauchecorne, A., Stepanov, A., Vinogradov, I., 2007b. A warm layer in Venus' cryosphere and high altitude measurements of HF, HCl, H_2O and HDO. Nature 450 (29), 646–649, doi:10.1038/nature05974.

Bertaux, J.-L., Vandaele, A.C., Wilquet, V., Montmessin, F., Dahoo, R., Villard, E., Korablev, O., Fedorova, A., 2008. First observation of 628 CO_2 isotopologue band at 3.3 mm in the atmosphere of Venus by solar occultation from Venus Express. Icarus 195 (1), 28–33.

Chamberlain, J.W., Hunten, D., 1987. Theory of Planetary Atmospheres: An Introduction to their Physics and Chemistry. Academic Press, New York.

Daerden, F., Whiteway, J.A., Davy, R., Verhoeven, C., Komguem, L., Dickinson, C., Taylor, P.A., Larsen, N., 2010. Simulating observed boundary layer clouds on Mars. Geophys. Res. Lett. 37, L04203.

Daerden, F., Chabrillat, S., Errera, Q., Bonjean, S., Fonteyn, D., Hoppel, K., Fromm, M., 2007. A 3d-ctm with detailed online psc-microphysics: analysis of the antarctic winter 2003 by comparison with satellite observations. Atmos. Chem. Phys. 7, 1755–1772.

Encrenaz, T., Bezard, B., Greathouse, T., Holmes, S., Richter, M., Nuccitelli, D., Lacy, J., Lebonnois, S., Lefèvre, F., Atreya, S., Wong, A., Owen, T., Forget, F., 2006. Ground-based high-resolution IR spectroscopy of Mars: H_2O and H_2O_2 mapping, search for CH_4, and determination of CO_2 isotopic ratios. In: MAMO Workshop, Granada.

Encrenaz, T., Bézard, B., Owen, T., Lebonnois, S., Lefèvre, F., Greathouse, T., Richter, M., Lacy, J., Atreya, S., Wong, A.-S., Forget, F., 2005. Infrared imaging spectroscopy of Mars: H_2O mapping and determination of CO_2 isotopic ratios. Icarus 179, 43–54.

Errera, Q., Daerden, F., Chabrillat, S., Lambert, J.-C., Lahoz, W.A., Viscardy, S., Bonjean, S., Fonteyn, D., 2008. 4D-Var assimilation of MIPAS chemical observations: ozone and nitrogen dioxide analyses. Atmos. Chem. Phys. 8 (61696187).

Fedorova, A., Korablev, O., Vandaele, A.C., Bertaux, J.-L., Belyaev, D., Mahieux, A., Neefs, E., Wilquet, V., Drummond, R., Montmessin, F., Villard, E., 2008. HDO and H_2O vertical distribution and isotopic ratio in the Venus mesosphere by SOIR spectrometer on board Venus Express. J. Geophys. Res., doi:10.1029/2008JE003146.

Formisano, V., Atreya, S., Encrenaz, T., Ignatiev, N., Giuranna, M., 2004. Detection of methane in the atmosphere of Mars. Science 306, 1758–1761.

Garcia Munoz, A., McConnell, J., McDade, I., Melo, S., 2005. Airglow on Mars: some model expectations for the OH Meinel bands and the O_2 IR atmospheric band. Icarus 176, 75–95.

Hase, F., Wallace, L., McLeod, S., Harrison, J.J., Bernath, P., 2009. The ACE-FTS atlas of the infrared solar spectrum. J. Quant. Spectrosc. Radiat. Transfer, doi:10.1016/j.jqsrt.2009.10.020.

Krasnopolsky, V., 1996. Oxygen and carbon isotope ratios in Martian carbon dioxide: measurements and implications for atmospheric evolution. Icarus 124 (2), 553–568.

Krasnopolsky, V., 2010. Atmospheric chemistry on Venus, Earth and Mars: main features and comparison. Planet. Space Sci. 2810, doi:10.1016/j.pss.2010.02.011.

Krasnopolsky, V., Maillard, J., Owen, T., 2004. Detection of methane in the Martian atmosphere: evidence for life? Icarus 172 (2), 537–547.

Lefevre, F., Bertaux, J., Clancy, R., Encrenaz, T., Fast, K., Forget, F., Lebonnois, S., Montmessin, F., Perrier, S., 2008. Heterogeneous chemistry in the atmosphere of Mars. Nature 454, 971.

Lefevre, F., Forget, F., 2009. Observed variations of methane on Mars unexplained by known atmospheric chemistry and physics. Nature 460, 720.

Lissauer, J., DePater, I., 2001. Planetary Sciences. Cambridge University Press, Cambridge, UK.

Lodders, K., Fegley, B., 1997. An oxygen isotope model for the composition of Mars. Icarus 126 (2), 373–394.

Mahieux, A., Berkenbosch, S., Clairquin, R., Fussen, D., Mateshvili, N., Neefs, E., Nevejans, D., Ristic, B., Vandaele, A.C., Wilquet, V., Belyaev, D., Fedorova, A., Korablev, O., Villard, E., Montmessin, F., Bertaux, J.-L., 2008. In-flight performance and calibration of SPICAV SOIR on board Venus Express. Appl. Opt. 47 (13), 2252–2265.

Mahieux, A., Wilquet, V., Drummond, R., Belyaev, D., Fedorova, A., Vandaele, A., 2009. A new method for determining the transfer function of an acousto optical tunable filter. Opt. Express 17, 2005–2014.

Moudden, Y., McConnell, J., 2005. A new model for multiscale modeling of the Martian atmosphere GM3. J. Geophys. Res. 110 (E04001, doi:10.1029/2004JE002354.

Mumma, M., Novak, R., DiSanti, M., Bonev, B., Dello Russo, N., Hewagama, T., Smith, M., 2004. Detection and mapping of methane and water on Mars. In: DPS Meeting, vol. 36. p. 1127.

Mumma, M., Villanueva, G., Novak, R., Hewagama, T., Bonev, B., DiSanti, M., Mandell, A., Smith, M., 2009. Strong release of methane on Mars in Northern Summer 2003. Science 323, 1041–1045.

Mumma, M., Villanueva, G., Novak, R., Hewagama, T., Bonev, B., DiSanti, M., Smith, M.D., 2007. Absolute measurements of methane on Mars: the current status. In: DPS Meeting, vol. 38. p. 471.

NASA, ESA, 2010. ExoMars Trace Gas Orbiter Instruments Investigations Announcement of Opportunity.

Neary, L., Daerden, F., Kaminski, J., McConnell, J.C., 2010. Mars methane emission and transport scenarios using the GEM-Mars GCM. In: EGU 2010.

Nevejans, D., Neefs, E., Van Ransbeeck, E., Berkenbosch, S., Clairquin, R., De Vos, L., Moelans, W., Glorieux, S., Baeke, A., Korablev, O., Vinogradov, I., Kalinnikov, Y., Bach, B., Dubois, J.-P., Villard, E., 2006. Compact high-resolution space-borne echelle grating spectrometer with AOTF based on order sorting for the infrared domain from 2.2 to 4.3 micrometer. Appl. Opt. 45 (21), 5191–5206.

Smith, M., 2004. Interannual variability in TES atmospheric observations of Mars during 1999–2003. Icarus 167, 148–165.

Vandaele, A.C., De Mazière, M., Drummond, R., Mahieux, A., Neefs, E., Wilquet, V., Belyaev, D., Fedorova, A., Korablev, O., Montmessin, F., Bertaux, J.-L., 2008. Composition of the Venus mesosphere measured by SOIR on board Venus Express. J. Geophys. Res., doi:10.1029/2008JE003140.

Vandaele, A.C., Wilquet, V., Mahieux, A., Perevalov, V., Tashkun, S., Fedorova, A., Korablev, O., Montmessin, F., Bertaux, J.L., 2007. First detection of the 01111-00001 band of 12C16O18O in the Venus atmosphere by SPICAV/SOIR. In: DPS meeting, vol. 39.

Whiteway, J.A., Komguem, L., Dickinson, C., Cook, C., Illnicki, M., Seabrook, J., Popovici, V., Duck, T., Davy, R., Taylor, P.A., Pathak, J., Fisher, D., Carswell, A.I., Daly, M., Hipkin, V., Tamppari, L., Renno, N., Moores, J., Lemmon, M., Daerden, F., Smith, H., 2009. Mars water ice clouds and precipitation. Science 325 (68).

Wilquet, V., Fedorova, A., Montmessin, F., Drummond, R., Mahieux, A., Vandaele, A.C., Villard, E., Korablev, O., Bertaux, J.-L., 2009. Preliminary characterization of the upper haze by SPICAV/SOIR solar occultation in UV to mid-IR onboard Venus Express. J. Geophys. Res. 114 (E00B42, doi:10.1029/2008JE003186.

Wilquet, V., Mahieux, A., Vandaele, A., Perevalov, V., Tashkun, S., Fedorova, A., Korablev, O., Montmessin, F., Dahoo, R., Bertaux, J.-L., 2008. Line parameters for the 01111-00001 band of 12C16O18O from SOIR measurements of the Venus atmosphere. J. Quant. Spectrosc. Radiat. Transfer 109, 895–905.